Dogs lap using acceleration-driven open pumping

Sean Gart[a], John J. Socha[a], Pavlos P. Vlachos[b], and Sunghwan Jung[a,1]

[a]Biomedical Engineering and Mechanics, Virginia Tech, Blacksburg, VA 24061; and [b]School of Mechanical Engineering, Purdue University, West Lafayette, IN 47907

Edited by David A. Weitz, Harvard University, Cambridge, MA, and approved November 9, 2015 (received for review July 27, 2015)

Dogs lap because they have incomplete cheeks and cannot suck. When lapping, a dog's tongue pulls a liquid column from the bath, suggesting that the hydrodynamics of column formation are critical to understanding how dogs drink. We measured lapping in 19 dogs and used the results to generate a physical model of the tongue's interaction with the air–fluid interface. These experiments help to explain how dogs exploit the fluid dynamics of the generated column. The results demonstrate that effects of acceleration govern lapping frequency, which suggests that dogs curl the tongue to create a larger liquid column. Comparing lapping in dogs and cats reveals that, despite similar morphology, these carnivores lap in different physical regimes: an unsteady inertial regime for dogs and steady inertial regime for cats.

drinking | lapping | open pumping | biomechanics

Animals that interact with an air–fluid interface have evolved highly specialized behaviors to deal with the physical challenge of crossing fluidic regimes. Archerfish adjust for index of refraction when shooting water jets through the interface to catch prey (1, 2), some marine copepods leap into the air to avoid predation (3–6), and lizards and frogs run or skip across the water surface to escape predators (7–9). However, almost all terrestrial animals interact regularly with the air–water interface when they drink or feed (10–22). These animals use a wide array of mechanisms to breach the interface and transport fluid into their bodies, including viscous dipping, capillary suction, viscous suction, licking, and lapping (17). For mammalian carnivores, their mechanisms for drinking are constrained by the anatomy of the oral apparatus: with incomplete cheeks, they cannot form a seal to suck fluids into the mouth, and instead use the tongue to lap up fluids (17, 19–22). Lapping is a behavior that is familiar to most pet owners worldwide, but its physical mechanism is only understood in felines (21), and the underlying physics of drinking by dogs remains unexplained.

When a dog laps, the tongue first extends, and is curled backward (ventrally) into a "ladle" shape. The curled tongue impacts the liquid surface, inducing a splash. The tongue then retracts into the mouth, and the cycle is completed when the jaws snap shut. During tongue retraction, fluid adheres to the dorsal side of the tongue and is pulled upward toward the mouth, forming a water column that extends from the bath (21, 22). Informal observations from previous studies (17, 21) have suggested that dogs scoop water with the ventral side of the tongue in the ladle, but recent X-ray imaging has shown that most of the scooped liquid falls off the tongue, and only liquid that sticks to the dorsal side of the tongue is transported to the throat (22). Based on the lack of the use of the curled tongue as a ladle, and general anatomical similarity, Crompton and Musinsky (22) concluded that dogs and cats share the same basic mechanism of drinking. However, the kinematics and the hydrodynamics of lapping by dogs have never been studied in detail, and it is possible that dogs and cats use different physical mechanisms to transport liquid, despite their similar morphologies. Here, we investigate the detailed hydrodynamics that enable lapping in dogs by addressing how inertial, gravitational, and surface tension forces govern the dynamics of water column formation by the tongue, and how column formation interacts with the relative timing of the lapping motion.

Results

Lapping Kinematics. To obtain the kinematics of lapping, we filmed 19 dogs drinking water. Dog types included mixed and purebred specimens, reflecting a phylogenetically diverse sampling (23). We hypothesized that tongue size and kinematics should vary with lapping performance. To track the motion of the tongue and measure its relevant dimensions of contact with the surface, we used two cameras, one placed outside the water bowl in a lateral view, and the other placed inside the bottom of the bowl looking upward (Fig. S1 and Movie S1). Image processing techniques were used to quantify tongue motion (see *Materials and Methods* for details) and effective tongue contact size was measured as the projected effective radius, R, onto the water surface, which ranged from 12 to 25 mm. Tongue radius scaled isometrically with body mass, M ($R \sim M^{1/3}$, Fig. S2).

Tongue length was measured as the straight-line distance from the mouth opening to the anteriormost point of the curled tongue (Fig. S3). Plots of tongue length and velocity through a lapping cycle for representative large and small dogs are shown in Fig. 1 *B* and *C*, which show that the dog extends its tongue into the water at a relatively low speed. However, when the tongue exits the water and returns to the mouth, high accelerations (1–4 g) and high speeds (0.7–1.8 m/s) were observed.

Such high accelerations contrast with those of domestic cats, which move their tongue upward at ∼1–2 g then decelerate the tongue as it enters the mouth (21). To determine the significance of unsteady inertial effects, we modeled the fluid transport as an open fluid pump (Fig. 4*B*), driven by a pressure difference between points A (on the tongue) and B (in the far field). Comparing the unsteady pressure to steady pressure terms gives the Strouhal number $St = 6R_A/(U_{max}T)$ (see *Materials and Methods* for details). For dogs, St = 3.7 ± 1.4 (mean ± SD) and for cats (21), St ∼ 1.1, indicating that unsteady effects drive the motion of the liquid column for dogs, but not for cats. Although both

Significance

Cats and dogs are assumed to drink similarly, but little is known about the actual physical mechanisms that dogs use to transport fluids when lapping. We observed the drinking behavior of a wide range of dogs across breeds and body size, and used physical experiments to mimic the motion of a dog's tongue as it exits the water. Dogs accelerate the tongue upward more quickly than do cats, and then time their bite to coincide with the pinch-off of the column. The everyday experience of dogs as messy drinkers results from the backward curl of the tongue, which increases the size of the water column and thus enables dogs to drink more per lap than with a straight tongue.

Author contributions: S.G., J.J.S., P.P.V., and S.J. designed research; S.G., J.J.S., P.P.V., and S.J. performed research; S.G. and S.J. analyzed data; and S.G., J.J.S., P.P.V., and S.J. wrote the paper.

The authors declare no conflict of interest.

This article is a PNAS Direct Submission.

[1]To whom correspondence should be addressed. Email: sunnyjsh@vt.edu.

This article contains supporting information online at www.pnas.org/lookup/suppl/doi:10.1073/pnas.1514842112/-/DCSupplemental.

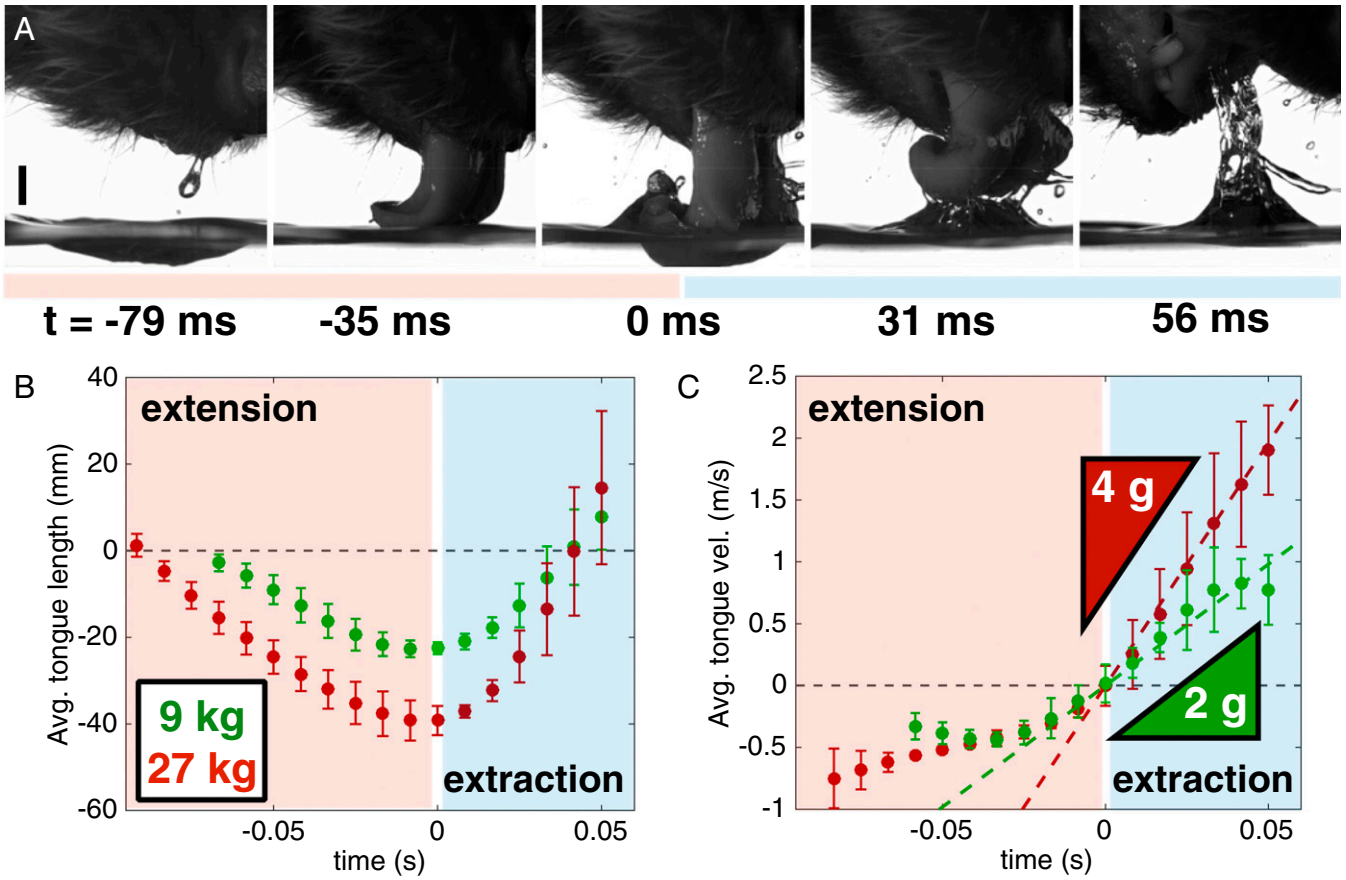

Fig. 1. Tongue kinematics of lapping dogs (also see Movie S1). (*A*) A dog (Labrador/poodle mix, 29.5 kg) extends and curls its tongue backward, strikes the surface of the fluid (time 0 is at maximum tongue length), and quickly withdraws its tongue to form a water column above the bath (recorded at 1,500 fps). (Scale bar, 10 mm.) The color bar corresponds to extension and retraction as in *B* and *C*. (*B*) Length versus time of four laps for a Shiba Inu (9 kg) and a Labrador mix (27 kg). The error bars represent 1 SD from four laps for each dog. Red shading denotes tongue extension and entry into the water, and blue shading denotes tongue exit and retraction back into the mouth. (*C*) Velocity versus time for the two dogs. The small dog's tongue has an acceleration of ~2 g, compared with the large dog's value of ~4 g. Comparison with cats can be made by referring to ref. 21.

animals use their tongues to lap, dissimilar tongue kinematics result in a significantly different interplay of forces, suggesting that cats and dogs use different physical mechanisms for drinking.

Two important questions remain to be answered. If dogs do not actually scoop water with the back of the tongue, why do they curl the tongue when they drink? And, what is the effect of high tongue acceleration on the water column formed by the tongue, relative to the timing of the lapping cycle?

Physical Experiment to Mimic Lapping. To address these questions and gather a deeper understanding of the hydrodynamics of lapping, we performed a physical experiment that simulates the hydrodynamics of liquid column formation using a rounded rod to simulate the tongue (Movie S2). The most crucial aspect of the lap appears to be the quick retraction of the tongue into the mouth, a motion that creates a water column that the dog drinks. In this experiment, we varied the upward acceleration and the size of the rod to capture the relevant physical regime used by drinking dogs. Dimensional analysis reveals high Reynolds $\mathcal{O}(10^3 - 10^4)$, Froude $\mathcal{O}(10^0 - 10^1)$, and Weber $\mathcal{O}(10^1 - 10^3)$ numbers, suggesting that viscous and capillary forces should be negligible compared with inertia and gravity. To confirm the insignificance of surface tension effects, both water ($\sigma = 72$ mN/m) and ethanol ($\sigma = 20$ mN/m) were used as a liquid bath.

Rounded glass rods ($R = 8$–20 mm) were positioned such that the tip was one radius below the surface of the bath, and then pulled out by stretched springs (see *Materials and Methods* for details), giving the rod a near-constant upward acceleration with magnitudes (1–8.5 g) that encompass the measured values from dogs (1–4 g). When the rod traveled up, a column of water was pulled out of the bath due to inertia, simulating the column formed by a dog's tongue (Fig. 2*A*). The extracted volume was measured from a distance $R/2$ above the bath to avoid the large bulk of liquid that quickly falls down (see Fig. S6).The volume of the column was measured through time and the moment of pinch-off was identified (open circles in Fig. 2*B*). The measured volumes of liquid extracted from the bath were on the same order of magnitude as the volume that a dog drinks per lap (~2.5 mL) (24). We found that the total volume of liquid extracted from the bath was positively correlated with rod size (see Fig. S7). This result suggests that a dog curls its tongue to increase the effective diameter in contact with fluid, extracting more fluid than if the tongue were withdrawn straight out of the bath.

From this physical experiment, we also see that the extracted volume is positively correlated with rod acceleration (Fig. S7), indicating that the dog could modulate tongue acceleration to control the amount of fluid that is pulled out of the bath. However, the tongue's maximum acceleration, and hence the maximum extracted volume per lap, is limited by biomechanical constraints. Fig. 2*B* shows that the pinch-off time of the fluid column largely depends on acceleration of the rod, with larger accelerations producing shorter pinch-off times. Thus, to optimize the volume ingested per lap, the dog should accelerate its tongue as fast as possible, while also timing its bite so that its jaws

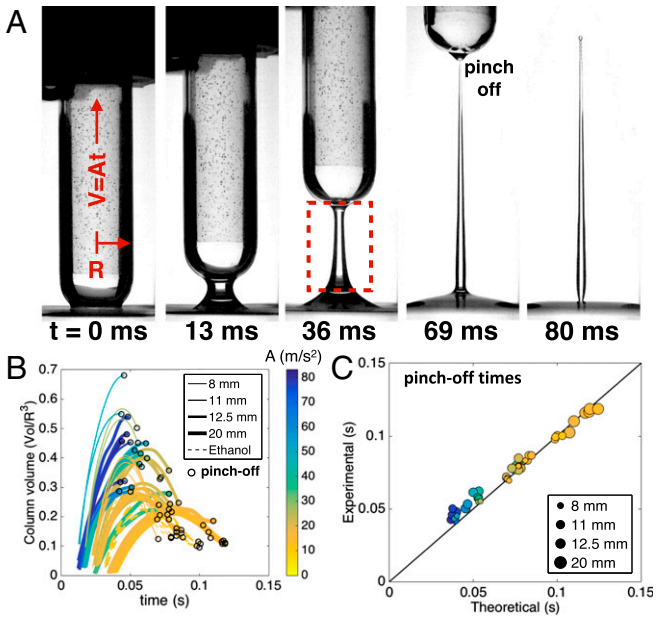

Fig. 2. Dynamics of water column formation in the physical rod experiment (also see Movie S2). (*A*) A rod ($R = 11$ mm) pulls liquid out of a bath with an acceleration of 1.6 g; the liquid then pinches off from the rod and falls back toward the bath. The red box shows where volume was measured $R/2$ above the surface for that frame. Pinch-off occurs at $t = 69$ ms. (*B*) Liquid volume in the column versus time as a rod was pulled out of the water ($n = 50$). Liquid volume was normalized by the radius of the rod cubed (vol/R^3) to compare across rod sizes. Line width corresponds to rod radius, color to acceleration, and dashed lines represent ethanol cases. The open circles represent the time of pinch-off. The curves are time-shifted so that $t = 0$ is the moment that the bottom of the rod was level with the fluid surface. (*C*) Experimental pinch-off time versus theoretical pinch-off time t_p^{theory} ($n = 50$). The black line has a slope of 1. Only rods with acceleration greater than 1 g are shown.

are closing at the moment of pinch-off. These actions are bounded by the jaw muscles' physiology and arrangement, and the relative sizes of the tongue and jaws (25, 26).

Comparison of Physical Experiment to Lapping Dogs. To compare the physical experiment to the dog's lapping behavior, we derived a theoretical scaling for the time for a water column to pinch off. Assuming that column dynamics are governed purely by the rod's acceleration, we find a pinch-off time, t_p^{theory}, that is inversely correlated to tongue acceleration: $t_p^{theory} \simeq \pi\sqrt{R/A}$, where R is rod radius and A is rod acceleration (see *Materials and Methods* for details). Fig. 2*C* shows that there is good agreement between experimental and theoretical pinch-off times, indicating that the theoretical model captures the physics of the physical model.

When does the pinch-off time occur relative to the dog's bite time? We defined the bite time, t_{close}, as the time between the tongue's exit from the water bath to when the jaw closes, measured from the lapping videos. From four laps per dog ($n = 4 \times 19$), we found that the ratio t_{close}/t_p^{theory} for all dogs is 0.92 ± 0.23 (mean $\pm$ SD, Fig. 3*A*), indicating that the dogs bit down on the water column approximately at pinch-off, which should maximize the intake of water per lap. This result provides the connection between the dog's drinking behavior and our physical model, and also leads us to predict the optimum frequency for lapping.

From Fig. 3*A*, we observe that $t_{close} \propto t_p^{theory}$, and if we assume $t_{close} \propto 1/f_{lap}$, then $t_p^{theory} \propto 1/f_{lap}$, and lapping frequency for dogs should scale as $f_{lap} \sim M^{-1/6}$, where M is the mass of the dog (see *Materials and Methods* for details). In a previous study (21), felines were shown to lap with this same scaling, determined using the assumption of steady inertia of the tongue with gravity. Because dogs exhibited unsteady inertia (high acceleration), it might make sense that the scaling would be different between cats and dogs. Surprisingly, our data show that the frequency scaling for dogs shows the same $M^{-1/6}$ trend as for cats (Fig. 3*B*).

Discussion

The results of this study help to explain the qualitative observations of many dog owners: Dogs tend to be messy drinkers and splash water on themselves and the floor. This phenomenon may be a by-product of their lapping mechanism. The large effective area of a dog's tongue that impacts the liquid surface, the penetration of the tongue below the liquid surface, and the high acceleration of the tongue as it is raised out of the liquid bath all contribute to increasing the volume of fluid extracted per lap. However, not all of the fluid displaced by the curled tongue enters the vertical column, and some is splashed laterally. In addition, when the tongue is accelerated upward, the water in the ladle is generally tossed to either side of the dog's mouth. Although dogs do not use their tongue to actively scoop water into their mouth, it is possible that the scooped liquid has some positive effect on the water column dynamics below the tongue. In particular, the scooped liquid could spill around the tongue and feed into the water column below, extending the formation time and increasing the volume of the column. This hypothesized role of scooping in the fluid column dynamics should be investigated further.

Materials and Methods

Animals. We used 19 dogs, which were volunteered for filming by pet owners from the local region (Table S1). We chose the dogs to span the diversity of "breeds" reflected in a modern phylogenetic analysis of dog relationships (23). A mixed or purebred dog from each major phenotypic designation (terms also used by breeders, e.g., "spaniels," "working dogs," "retrievers," etc.) except for wolves was represented. The owners provided the weight and breed of dogs at the time of filming. Animal experiments were approved by the Virginia Tech Animal Care and Use Committee (protocol #13-014-ME).

Filming of Dogs. Dogs were filmed drinking water naturally from a rectangular acrylic container using two GoPro cameras (Hero 3+ Silver, GoPro) at 120 frames per second (fps) (Movie S1, image size: 1,280 × 720 pixels). One camera was placed outside of the container and the other beneath or in the bottom of the container (Fig. S1). Only natural light was used, with no external lighting. Thirteen dogs were filmed outdoors at their owners' residences in the region of Blacksburg, VA, and the remaining six were filmed outdoors on the campus of Virginia Tech, Blacksburg, VA. If dogs refused to drink, they were lightly exercised by going on a 5-min run or walk with their owners and then brought back to the water container to drink. Dogs drank voluntarily or did not drink at all. No other fluid besides water was placed in

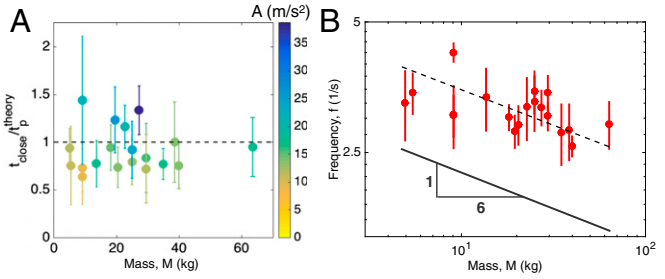

Fig. 3. Comparison of column pinch-off times and lapping frequency versus mass for dogs. (*A*) Jaw closing time over theoretical pinch-off time for all dogs ($n = 4 \times 19$). (*B*) Frequency of lapping versus weight for dogs. $f_{lap} \sim M^{-1/6}$ is shown with the gray solid line. The line of best fit (dashed black) has slope -0.16 ± 0.09 (95% CI). For both *A* and *B*, error bars indicate the SD for each dog (4 laps × 19 dogs).

the drinking containers. For Fig. 1*A*, a high-speed camera (APX-RS, Photron) recorded the dog at 1,500 fps with backlighting in a laboratory at Virginia Tech. Two dogs were recorded with the Photron camera; eight lapping sequences were recorded with a duration from 0.8 to 4.1 s, with 2–12 laps per sequence.

The projected tongue effective radius was measured from video stills from the bottom-view camera (Fig. S2) using MATLAB image processing techniques. Tongue length was measured from the mouth opening to the bottom of the "scooped" part of the tongue (Fig. S3*A*). The bottom of the curved part of the tongue was chosen as the end point because it remained in contact with the water throughout the lap, and is analogous to the bottom tip of the rod. Motion of the tongue was measured by digitizing two points on each frame and measuring the distance between them until the tongue was no longer visible in the mouth. Once the tongue passed the mouth opening, which was defined by a line drawn between the nose and the tip of the bottom of the jaw, it was considered to have positive length, such that there was a positive tongue velocity when the tongue was moving up into the mouth. Instantaneous tongue velocity was calculated as the difference in length between successive frames. To find tongue acceleration, a first-order polynomial function was fit to the velocity data using least-squares regression, using points from the minimum velocity (when the tongue is at full extension) to the maximum velocity (as the tongue enters the mouth). This slope fitting was done to avoid potentially large errors that occur from numerical differentiation (27). Tongue length and velocity versus time for all dogs is shown in Fig. S4.

To determine the significance of unsteady versus steady inertia effects on the lapping mechanics, we considered a reduced-order model (Fig. 4*B*). From our experiments, we found that the major mechanism of transport is inertia. Therefore, assuming high Reynolds number and neglecting surface tension, the flow can be considered as a potential flow, and can be written as $p_A - p_B \simeq -\rho R_A \partial u/\partial t - 1/2\rho u^2$, where p is pressure, ρ is fluid density, R_A is the tongue radius, and u is the fluid velocity. With the accelerating tongue, the unsteady inertia scales as $\rho R_A du/dt \simeq \rho R_A U_{max}/T$, where T is the time from the minimum tongue velocity to the end of the lap and U_{max} is the maximum tongue velocity. Then, the effect of the steady inertia scales as $1/2\rho u^2 \simeq 1/2\rho\, U_{max}^2/3$, where the 1/3 factor is due to averaging of the velocity ($u = At$) over time. To pump, $p_A - p_B$ must be less than zero. A ratio of unsteady to steady effects scales as $6R_A/(U_{max}T)$, which is defined as the Strouhal number.

Physical Experiment. To simulate the dog's tongue, glass test tubes (Ace Glass Inc.) with rounded bottoms and radii of 8, 11, 12.5, and 20 mm were used. Springs were attached to linear sliders, which served to move the rods upward with a near-constant acceleration. To vary acceleration, springs of varying strength were used, and stretching length was also varied. A schematic of the experimental setup can be seen in Fig. S5. To track the upward motion of the rods, a randomly generated dot pattern was placed inside the tube and the MATLAB image processing toolbox automatically tracked the rod motion using image cross-correlation. The volume of fluid pulled from the bath was also measured with the MATLAB image processing toolbox. The motion of the rod and fluid was recorded using a high-speed camera (N3, Integrated Design Tools) at 1,500 fps and a shutter speed of 100–200 μs. The range of experimental parameters was R = 8, 11, 12.5, and 20 mm, A = 10–83 m/s^2, and surface tension σ = 20 mN/m (ethanol) and σ = 72 mN/m (water). The volume of the water column was measured from $R/2$ above the liquid surface to the bottom tip of the rod. This was to avoid the large bulk of liquid that barely rises out of the bath and quickly falls back down, as seen in Fig. S6. This analysis is justified because the dog is not able to drink this portion of the liquid; instead, it falls back to the bath well before the dog bites down on the column. We define time 0 (Fig. S6) as the time when the tip of the rod was level with the surface of the liquid bath. As seen in Fig. S7, the maximum volume extracted by a rod was positively correlated with the size and acceleration of the rod.

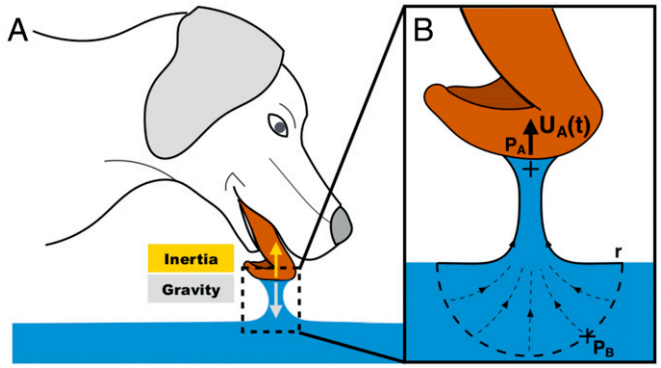

Fig. 4. Schematic of the competition between inertia and gravity during a lap, modeled in the rod experiment. (*A*) Schematic depicting the opposition of inertia and gravity during lapping. (*B*) A model of open pumping, developed to understand how the dog creates a water column. In this model, the pressure difference between points A and B drives the extraction of fluid from the bath. Point A is beneath the tongue (indicated with a plus sign), point B is considered at a far field $r \to \infty$, and $U_A(t)$ is the tongue velocity.

Scaling Analysis for Pinch-Off Time, t_p^{theory}. For all trials, we observed that pinch-off occurred very close to the tip of the rod. The velocity potential in fluid column due to the acceleration rod can be estimated as $\phi \sim RAt$. Using the unsteady Bernoulli relation, the radial velocity is obtained to be $v_R \sim \sqrt{AR}$. To start, the equation for the wetted length on the rounded end of the cylinder is $s(t) \simeq \pi R - \int_0^t v_R dt$, where R is the radius of the rod, v_R is the radial velocity of the water column, and t is the time since the rod tip exited the fluid bath. πR is used as the initial distance because the contact line of the fluid with the rod must travel along the curved portion of the rod before pinch-off. The pinch-off time was determined when $s(t_p^{theory}) = 0$. The radial velocity is then inserted into the expression for $s(t)$ to get $t_p^{theory} = \pi\sqrt{R/A}$. This pinch-off scaling has also been confirmed previously (28); however, their experiments were in the stretching regime where surface tension dominates. From Fig. 2*C*, it can be seen that our theoretical equation for pinch-off time, $t_p^{theory} = \pi\sqrt{R/A}$, matches well with experimental data in which there is high acceleration of the rod (above ~1 g).

A Second Scaling Analysis for Pinch-Off Time, $t_p^{theory,2}$. We have also developed another theoretical relationship for low accelerations based on the pressure difference in the column pulled from a bath (21). Similarly, the liquid column on the cylinder follows $s(t) \simeq \pi R - \int_0^t v_R dt$. If we assume that hydrostatic pressure drives the motion of the column interface, v_R can be written as $v_R \sim \sqrt{gH}$, where H is the height of the tip of the rod above the free surface and g is acceleration due to gravity (21). The rod moves with a constant acceleration, so $H = 1/2At^2$, where A is acceleration of the rod. Pinch-off occurs when $s(t)$=0, so the equation becomes $0 \simeq \pi R - \int_0^{t_p} \sqrt{1/2gAt^2}dt$. Solving for t_p gives $t_p^{theory,2} = (2\sqrt{2}\pi R)^{1/2}/(Ag)^{1/4}$. $t_p^{theory,2}$ overpredicts the pinch-off time for a dog's lap at high accelerations, but it matches experimental data well for rods with small accelerations. We believe that t_p^{theory} is valid for the dogs, as dogs lap with large tongue acceleration (1–4 g). Fig. S8 shows a comparison between the two theoretical equations for pinch-off and that t_p^{theory} matches the data well for acceleration above 1 g. In this figure, both t_p^{theory} (blue line) and $t_p^{theory,2}$ (black line) have no fitting parameters.

Scaling Analysis of the Maximum Column Volume. First, we consider the time scale of the maximum column volume. The column volume increases due to upward acceleration, and drains due to gravity. If a control volume is chosen for the liquid column, there are two pressures competing with one another: one is the pressure due to unsteady motion ($\rho\partial\phi/\partial t \sim \rho AR$), and the other is pressure due to gravity ($\sim \rho gH$), where H is the height of the column. The height of the column increases as $H \sim 1/2At^2$. These two forces are balanced at $t_{grav} = \sqrt{R/g}$. Rescaling time by t_{grav} gives the time of maximum volume at t_{grav} = 1.6 ± 0.2 (mean ± SD).

Next we consider the volume of the liquid column. The liquid column can be considered as a conical shape, as observed in our experiments. Also, when the liquid column reaches its maximum volume, the height of the conical shape is close to the height of the rod (as shown in Fig. S7*C*). To start, we use two assumptions: that the liquid column has a conical shape with height H and that the bottom of the liquid column has radius R (the rod size). From our physical experiments, we observed that for high accelerations, the column has maximum volume at pinch-off, and for low accelerations, maximum volume occurs before pinch-off. Comparing t_{grav} with t_p^{theory} gives $\pi\sqrt{R/A} \sim 1.6\sqrt{R/g}$, and the transition from low to high acceleration is identified. When $A/g < \pi^2/1.6^2$, the column reaches maximum volume before pinch-off, and the maximum volume is $V_0 = (\pi/3)R^2H$, where $H = 1/2At^2$. Then, $V_0 = (\pi/6)R^3(A/g)(1.6)^2$ at $t = t_{grav}$. When $A/g > \pi^2/1.6^2$, column volume is maximum at pinch-off and $V_0 = (1/6)R^3\pi^2$ at $t = t_p^{theory}$. This scaling is shown in Fig. S7 *A* and *B*. Although the scaling works fairly well, there are some sources of error that cause inconsistencies. The bottom radius of the

column is not always close to the rod radius at time of maximum volume or pinch-off. There could also be some surface tension effects that influence column volume that we do not take into account.

Derivation of Frequency Scaling for Dogs. From Fig. 3*A*, the dog's jaw closing time, t_{close}, is proportional to the rod pinch-off time, t_{pinch}. Jaw closing time, t_{close}, is also proportional to $1/f_{lap}$, where f_{lap} is lapping frequency: $1/f_{lap} \propto \sqrt{R/A}$. From Fig. S2, tongue radius scales as $R \sim M^{1/3}$ to give $f_{lap} \sim A^{1/2} M^{-1/6}$. There is also no significant relationship between A and any other parameter, so we assume that A is insignificant with respect to dog mass, tongue radius, and lapping frequency (R^2 of 0.058, 0.19, and 0.000040, respectively), which gives $f_{lap} \sim M^{-1/6}$.

ACKNOWLEDGMENTS. The authors thank Dr. Stephen Childress for inspiring discussion, Thomas Magelinski and Talia Weiss for their assistance, and two anonymous reviewers for comments that helped to improve the paper. This research was supported by the National Science Foundation (PoLS-1205642 to S.J., J.J.S., and P.P.V.; CBET-1336038 to S.J. and P.P.V.; and IDBR-1152304 to P.P.V. and J.J.S.).

1. Lüling K (1963) The Archer fish. *Sci Am* 209(1):100–109.
2. Gerullis P, Schuster S (2014) Archerfish actively control the hydrodynamics of their jets. *Curr Biol* 24(18):2156–2160.
3. Buskey E, Lenz P, Hartline D (2002) Escape behavior of planktonic copepods in response to hydrodynamic disturbances: High speed video analysis. *Mar Ecol Prog Ser* 235:135–146.
4. Waggett RJ, Buskey EJ (2007) Calanoid copepod escape behavior in response to a visual predator. *Mar Biol* 150(4):599–607.
5. Gemmell BJ, Jiang H, Strickler JR, Buskey EJ (2012) Plankton reach new heights in effort to avoid predators. *Proc R Soc B* 279(1739):2786–2792.
6. Kim SJ, Hasanyan J, Gemmell BJ, Lee S, Jung S (2015) Dynamic criteria of plankton jumping out of water. *J R Soc Interface* 12(111):20150582.
7. Glasheen J, Mcmahon T (1996) Size-dependence of water-running ability in basilisk lizards (*Basiliscus basiliscus*). *J Exp Biol* 199(Pt 12):2611–2618.
8. Bush JWM, Hu DL (2006) Walking on water: Biolocomotion at the interface. *Annu Rev Fluid Mech* 38(1):339–369.
9. Gans C (1976) The process of skittering in frogs. *Ann Zool* 12(2):37–40.
10. Weijnen JAWM (1998) Licking behavior in the rat: measurement and situational control of licking frequency. *Neurosci Biobehav Rev* 22(6):751–760.
11. Bennet-Clark HC (1963) Negative pressures produced in the pharyngeal pump of the blood sucking bug, *Rodnius prolixus*. *J Exp Biol* 40(1):223–229.
12. Berkhoudt H, Kardong KV, Zweers GA (1995) Mechanics of drinking in the brown tree snake, *Boiga irregularus*. *Zoology* 98(2):92–103.
13. Kim W, Gilet T, Bush JWM (2011) Optimal concentrations in nectar feeding. *Proc Natl Acad Sci USA* 108(40):16618–16621.
14. Rico-Guevara A, Rubega MA (2011) The hummingbird tongue is a fluid trap, not a capillary tube. *Proc Natl Acad Sci USA* 108(23):9356–9360.
15. Kingsolver JG, Daniel TL (1979) On the mechanics and energetics of nectar feeding in butterflies. *J Theor Biol* 76(2):167–179.
16. Prakash M, Quéré D, Bush JWM (2008) Surface tension transport of prey by feeding shorebirds: The capillary ratchet. *Science* 320(5878):931–934.
17. Kim W, Bush JWM (2012) Natural drinking strategies. *J Fluid Mech* 705(1):7–25.
18. Rico-Guevara A, Fan TH, Rubega MA (2015) Hummingbird tongues are elastic micropumps. *Proc Biol Sci* 282(1813):20151014.
19. Thexton AJ, Crompton AW, German RZ (1998) Transition from suckling to drinking at weaning: A kinematic and electromyographic study in miniature pigs. *J Exp Zool* 280(5):327–343.
20. Thexton AJ, McGarrick JD (1988) Tongue movement of the cat during lapping. *Arch Oral Biol* 33(5):331–339.
21. Reis PM, Jung S, Aristoff JM, Stocker R (2010) How cats lap: Water uptake by *Felis catus*. *Science* 330(6008):1231–1234.
22. Crompton AW, Musinsky C (2011) How dogs lap: Ingestion and intraoral transport in *Canis familiaris*. *Biol Lett* 7(6):882–884.
23. Vonholdt BM, et al. (2010) Genome-wide SNP and haplotype analyses reveal a rich history underlying dog domestication. *Nature* 464(7290):898–902.
24. Adolph EF (1938) Measurements of water drinking in dogs. *Am J Physiol* 125(1):75–86.
25. Westneat MW (2003) A biomechanical model for analysis of muscle force, power output and lower jaw motion in fishes. *J Theor Biol* 223(3):269–281.
26. Bates KT, Falkingham PL (2012) Estimating maximum bite performance in *Tyrannosaurus rex* using multi-body dynamics. *Biol Lett* 8(4):660–664.
27. Walker JA (1998) Estimating velocities and accelerations of animal locomotion: A simulation experiment comparing numerical differentiation algorithms. *J Exp Biol* 201(7):981–995.
28. Vincent L, Duchemin L, Villermaux E (2014) Remnants from fast liquid withdrawal. *Phys Fluids* 26(3):031701.

Supporting Information

Gart et al. 10.1073/pnas.1514842112

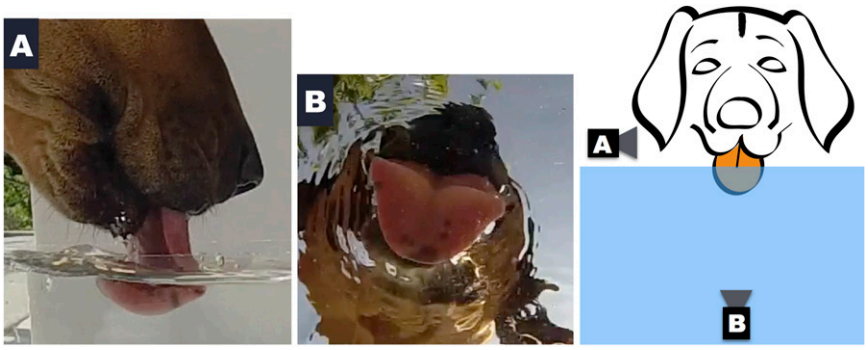

Fig. S1. Camera position during filming of lapping. Two video cameras (GoPro Hero 3+) were used to film the lapping of dogs. One camera was placed to the side (*A*), and the other camera was placed inside the water bowl facing upward (*B*). The side view (*A*) was used to measure tongue kinematics, and the bottom view (*B*) was used to measure the size of the tongue in contact with the water bath. Dogs were filmed outdoors in natural light at 120 frames per second (fps) and 720p format (resolution, 1,280 × 720 pixels).

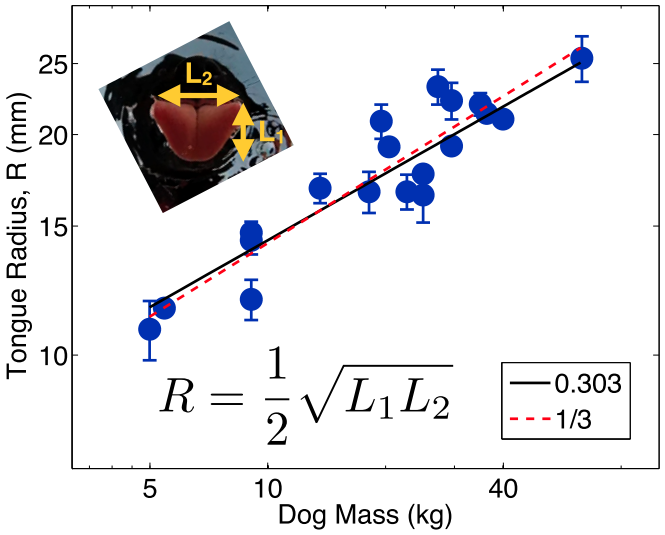

Fig. S2. Scaling of tongue size with body mass. The tongue radius scaled as $R \sim M^{0.303}$ (black line) with 95% CI of the slope of 0.077 ($n = 19$). Therefore, we assume that the tongue scales isometrically ($R \sim M^{1/3}$, red dotted line). The effective tongue radius (a proxy for tongue size) was calculated as one-half the square root of the width (L_2) multiplied by the height (L_1).

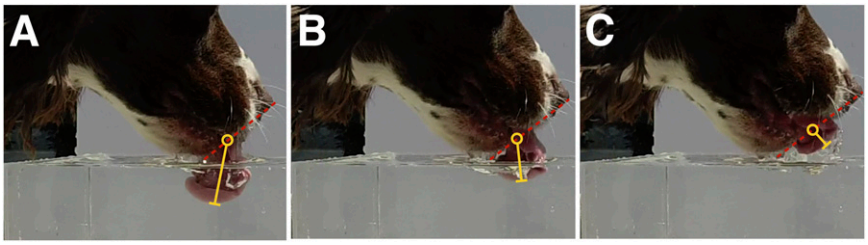

Fig. S3. How tongue length was measured; (*A*) $t = 0$, (*B*) $t = 25$ msec, and (*C*) $t = 42$ msec. The yellow line shows how tongue length was measured for three frames of drinking. The red dashed line drawn from the tip of the nose to the bottom jaw was used to define a zero tongue length. Once the tongue passes the red line into the mouth, it was defined to have a positive length. This is done so that there is a positive velocity when the tongue is moving upward and into the mouth. The part of the rounded tongue that is farthest from the jaw opening was chosen for the length, analogous to the tip of the rod in the physical experiment.

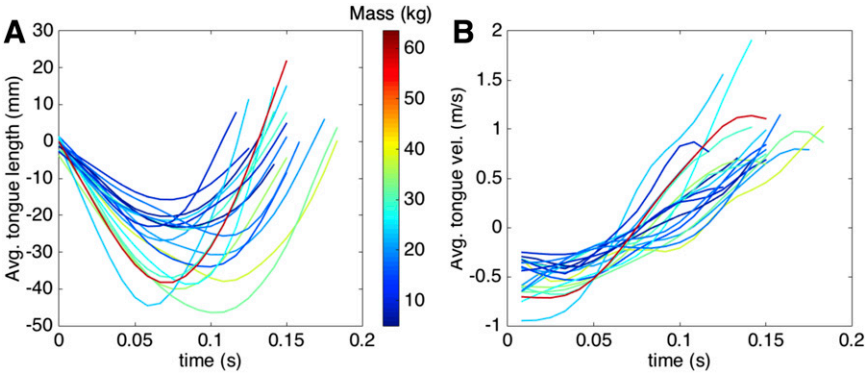

Fig. S4. Tongue length (*A*) and velocity (*B*) versus time for all dogs. The color coding corresponds to each dog's weight in kilograms. These plots show that the tongue entered the water bath at a relatively constant speed and then accelerated out of the bath and into the mouth. Velocity is negative when the tongue is moving down into the water, and positive when the tongue is moving back into the dog's mouth. Each line represents the average of four laps per dog ($n = 19$), and error bars are not shown for clarity.

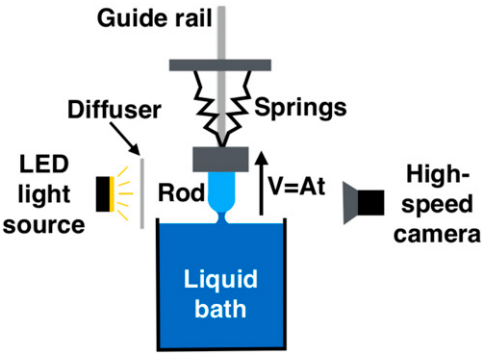

Fig. S5. Setup of the physical experiment. Glass rods were pulled upward by two stretched springs. The strength of the springs as well as the initial stretched length were varied to vary the resulting acceleration. A pulley system was used to pull the rod down into the bath and stretch the springs. Lubricated steel guide rails prevented any lateral motion of the rod. To accurately track the rod's motion, a random dot pattern was placed inside the rod. An IDT N3 high-speed camera recorded the motion at 1,500 fps with a shutter speed of 100–200 μs.

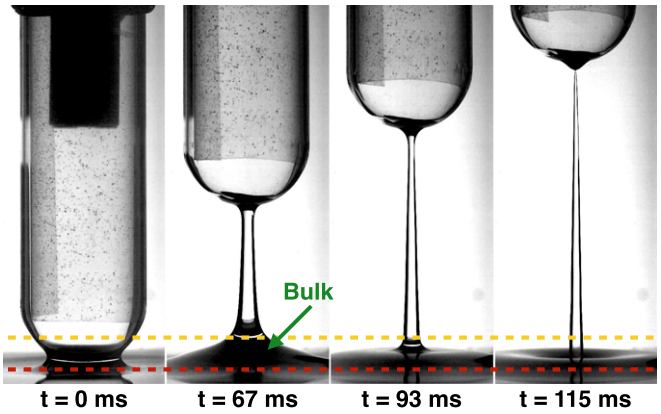

Fig. S6. Example of the large bulk that was excluded from volume calculations. An image sequence showing the large bulk that rises and falls back to the bath. The red dashed line indicates the fluid surface and the yellow dashed line is *R*/2 above the surface. Because the fluid quickly falls back into the bath, we did not include the liquid below the yellow line in our volume calculations.

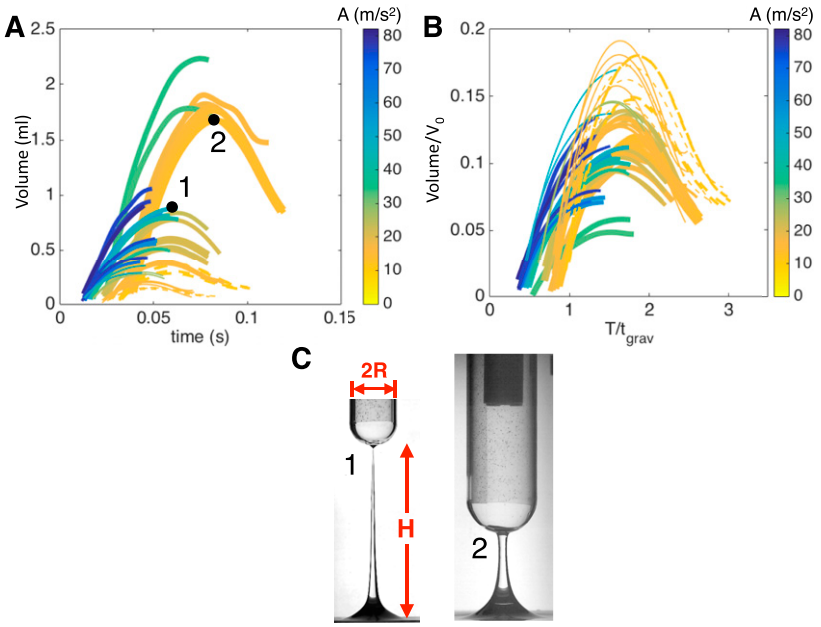

Fig. S7. Development of the water column through time. (*A*) Absolute volume of water in the developing column through time from the physical experiment. (*B*) Comparison of water column development using rescaled values. Column volume is normalized by the maximum theoretical volume, V_0, and time is normalized by $t_{grav} = \sqrt{R/g}$ (see *Materials and Methods* for details). The maximum volume occurs at 1.6 ± 0.2 of the rescaled time. (*C*) Examples of how the water column was approximated as a cone with height *H* and bottom radius *R* (same as the rod radius) for (1) a high-acceleration case (A = 44 m/s^2, *R* = 12.5 mm) where maximum volume occurs at pinch-off, and (2) a low-acceleration case (A = 11 m/s^2, *R* = 20 mm) where maximum volume occurs before pinch-off.

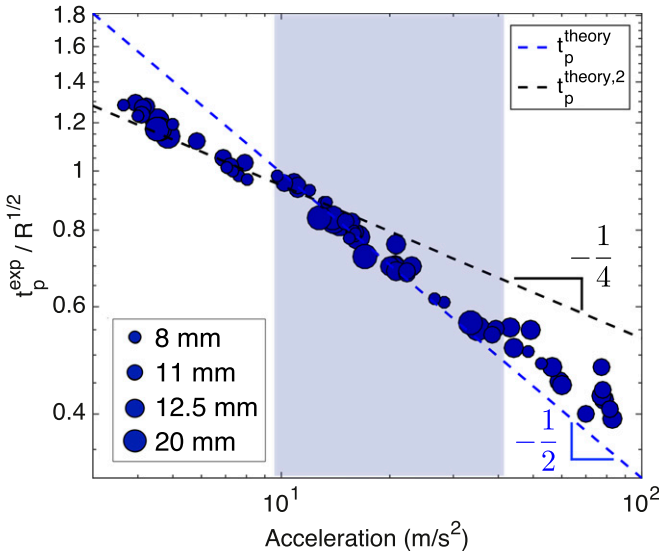

Fig. S8. Comparison of experimental pinch-off times with theory. Physical experiment pinch-off time, t_p^{exp}, over $R^{1/2}$ as a function of acceleration ($n = 70$). The blue dotted line shows $t_p^{theory} = \pi\sqrt{R/A}$ and the black dotted line shows $t_p^{theory,2} = (2\sqrt{2}\pi R)^{1/2}/(Ag)^{1/4}$. At high accelerations, t_p^{theory} slightly underpredicts the pinch-off time, whereas $t_p^{theory,2}$ overpredicts pinch-off time at high accelerations. t_p^{theory} is more valid for regime used by the dogs (blue color band).

Table S1. Sex, breed, and weight of all dogs used in the study

Number	Sex	Breed	Weight, kg
1	F	Mixed (boxer)	20
2	F	Mixed (Whippet)	9
3	F	Mixed (Labrador)	25
4	F	Brittany	25
5	F	Mixed (German shepherd, Belgian Malinois)	35
6	F	Mixed (unknown)	14
7	M	Mixed (Labrador, pit bull)	27
8	F	Mixed (Golden retriever, poodle)	40
9	M	Mixed (Labrador, poodle)	29
10	F	Mixed (Yorkshire terrier, Bichon frise)	5
11	F	Mixed (hound)	30
12	F	Mixed (cocker spaniel, poodle)	9
13	F	Portuguese water dog	23
14	M	Rottweiler	39
15	F	Shiba Inu	9
16	M	Border collie	18
17	M	Mixed (miniature pinscher)	5
18	F	Mixed (Labrador, terrier)	20
19	M	Great Dane	64

Movie S1. This movie shows the lapping of both the 9-kg and 27-kg dog from Fig. 1 *B* and *C*, filmed from the side and below with GoPro Hero 3+ video cameras at 120 fps. The videos are played at 1/4 speed.

Movie S1

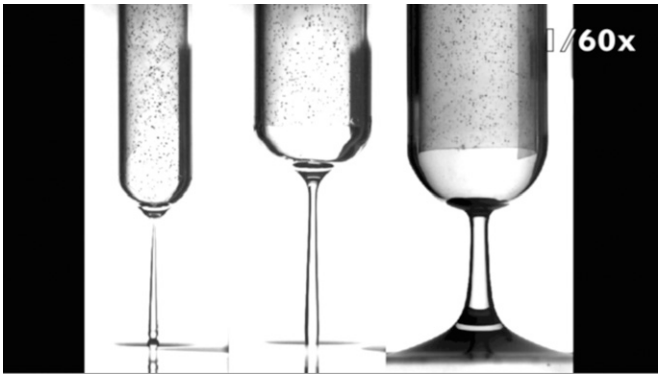

Movie S2. This movie shows an example of three rods of radius 8, 11.5, and 20 mm being pulled out of a bath in the physical experiment. The rods were accelerating at ∼1 g.

Movie S2